

ARTICLE

EDP-297: A novel, farnesoid X receptor agonist—Results of a phase I study in healthy subjects

Christine Marotta¹ | Alaa Ahmad¹ | Ed Luo¹ | Jart Oosterhaven² |
Sjoerd van Marle² | Nathalie Adda¹

¹Enanta Pharmaceuticals, Inc.,
Watertown, Massachusetts, USA

²ICON/PRA, Groningen, The
Netherlands

Correspondence

Alaa Ahmad, Enanta Pharmaceuticals
Inc., 400 Talcott Ave, Watertown, MA
02472, USA.

Email: aahmad@enanta.com

Abstract

EDP-297 is a farnesoid X receptor agonist under development for treating non-alcoholic steatohepatitis. The pharmacokinetic (PK), pharmacodynamic (PD), food effect, and safety were evaluated in a single ascending dose (SAD) and multiple ascending dose (MAD) phase I study. Healthy subjects received single EDP-297 doses of 20–600 µg or once daily doses of 5–90 µg for 14 days. Safety, PKs, and PDs were assessed, including fibroblast growth factor 19 (FGF-19) and 7- α -hydroxy-4-cholesten-3-one (C4). Among 82 subjects, EDP-297 was generally well-tolerated. Pruritus was observed in four subjects in the SAD phase and seven subjects in the MAD phase; four severe cases occurred at 90 µg in the MAD phase, including one that led to drug discontinuation. A grade 2 elevation in alanine aminotransferase occurred with 90 µg. Mean lipid values remained within normal range. Plasma exposures of EDP-297 increased with SADs and MADs, with mean half-life following multiple doses of 9–12.5 h. No food effect was observed. Mean FGF-19 increased and C4 decreased up to 95% and 92%, respectively. EDP-297 was generally well-tolerated up to 60 µg MAD, with linear PKs suitable for once daily oral dosing, target engagement, and no food effect.

Study Highlights**WHAT IS THE CURRENT KNOWLEDGE ON THE TOPIC?**

EDP-297 is a selective steroidal noncarboxylic farnesoid X receptor agonist under development for treating nonalcoholic steatohepatitis (NASH). In vitro studies have shown that EDP-297 modulates multiple pathways associated with the pathogenesis of NASH.

WHAT QUESTION DID THIS STUDY ADDRESS?

This first-in-human phase I study evaluated the pharmacokinetic (PK), pharmacodynamic, food effect, and safety of EDP-297 in a single ascending dose (SAD) and multiple ascending dose (MAD) trial.

WHAT DOES THIS STUDY ADD TO OUR KNOWLEDGE?

Plasma exposures of EDP-297 increased with SADs and MADs, with mean half-life following multiple doses of 9–12.5 h that supports once daily dosing. Further,

This is an open access article under the terms of the [Creative Commons Attribution-NonCommercial-NoDerivs](https://creativecommons.org/licenses/by-nc-nd/4.0/) License, which permits use and distribution in any medium, provided the original work is properly cited, the use is non-commercial and no modifications or adaptations are made.

© 2022 Enanta Pharmaceuticals Inc. *Clinical and Translational Science* published by Wiley Periodicals LLC on behalf of American Society for Clinical Pharmacology and Therapeutics.

no effect of food on the PK profiles was observed. Mean fibroblast growth factor 19 levels increased and 7- α -hydroxy-4-cholesten-3-one (C4) levels decreased up to 95% and 92%, respectively.

HOW MIGHT THIS CHANGE CLINICAL PHARMACOLOGY OR TRANSLATIONAL SCIENCE?

EDP-297 was generally well-tolerated with a linear PK profile with no food effect and is suitable for once daily oral dosing. EDP-297 also demonstrated target engagement consistent with a potent effect on the farnesoid X receptor and may be a promising treatment for NASH.

INTRODUCTION

Bile acids (BAs) play a key role in regulating liver and metabolic homeostasis, including regulation of lipid and glucose metabolism, which is mediated through two receptor pathways, farnesoid X receptor (FXR) and transmembrane G-protein-coupled receptor 5.^{1,2} The FXR is a ligand-activated nuclear hormone receptor that is expressed in the liver, gall bladder, gut, and kidneys.³ Activation of FXR by BAs modulates the expression of multiple gene-encoding proteins involved in BA biosynthesis, transport, and metabolism.^{3,4} In addition to regulation of BA homeostasis, FXR agonists exhibit anti-inflammatory and antifibrotic activity through suppression of nuclear factor kappa-light-chain-enhancer of activated B cell and transforming growth factor β signaling, respectively, and decrease liver triglyceride synthesis through blockade of sterol regulatory-element binding protein signaling.⁵⁻⁸ Hepatic expression of FXR is decreased in patients with nonalcoholic fatty liver disease (NAFLD), which is associated with hepatic triglyceride accumulation and hepatic steatosis, hyperlipidemia, hyperglycemia, BA overload, inflammation, and fibrosis.⁹ Moreover, studies have shown that these metabolic dysfunctions can be improved by FXR activation.¹⁰⁻¹²

EDP-297 is a selective steroidal noncarboxylic agonist of the FXR nuclear receptor subfamily 1, group H4 (NR1H4).¹³⁻¹⁵ Multiple cell-based assays demonstrate that EDP-297 dose-dependently transactivates FXR, regulates the expression of prototypic FXR genes, such as small heterodimer partner (NR0B2), and modulates multiple pathways associated with the pathogenesis of nonalcoholic steatohepatitis (NASH). In vitro and in vivo data suggest that the pharmacologic profile of EDP-297 is consistent with that of an agonist of FXR.^{16,17} In vitro data show that EDP-297 is a CYP3A4 substrate and is not a substrate of glucuronosyltransferase. Hepatic metabolism is expected to be the main route of metabolism.

This first-in-human study was undertaken to evaluate the safety/tolerability, pharmacokinetics (PKs), and

pharmacodynamics (PDs) of EDP-297 in a single ascending dose (SAD) phase and a multiple ascending dose (MAD) phase in healthy subjects and to determine the effect of food on the PKs of EDP-297.

METHODS

The study was conducted in compliance with the International Conference on Harmonization- Good Clinical Practices guidelines, the Declaration of Helsinki, and national regulations for clinical trials. The study protocol and informed consent were reviewed and approved by an Ethics Committee (Evaluation of Ethics in Biomedical Research, HK Assen, The Netherlands). Written informed consent was obtained from all participants prior to any study procedures. The study was conducted at PRA Health Sciences, Groningen, The Netherlands, and was registered at clinicaltrials.gov: NCT04559126.

Study design

This was a phase I, randomized, double-blind, placebo-controlled, first-in-human study to evaluate the safety, tolerability, PKs, and PDs during fasted and fed states, and of SADs and MADs of EDP-297 in healthy subjects (Figure S1). In the SAD phase, subjects were randomized in a 3:1 ratio to receive a single dose of EDP-297 at 20, 60, 100, 300, or 600 μ g or placebo. The SAD phase also included a fed cohort, where subjects were randomized in a 4:1 ratio to receive a single dose of EDP-297 100 μ g or placebo. Subjects in the fed cohort were given a standardized high fat content meal at a maximum of 30 min prior to their dose of study drug and study drug had to be administered within 10 min of completion of the meal (Table S1). The MAD phase was initiated after the completion of the SAD fed cohort so the fed/fasting status could be determined for the MAD phase. In the MAD phase, subjects were randomized to placebo or EDP-297 at doses of 5, 15,

30, 60, or 90 µg once daily (q.d.) for 14 days. Subjects in fasting cohorts fasted for at least 8 h overnight until 1 h postdose; water was permitted except for 1 h before and 1 h after dosing.

All dose escalations were determined after review of safety data prior to administering the subsequent cohort. The first SAD cohort (20 µg) was divided into two dosing groups; the first group (the sentinel group) included two subjects (1 active and 1 placebo) and the second group included the remaining six subjects (5 active and 1 placebo). The second group was dosed after assessment of 24-h safety data was completed for the sentinel group, and no significant safety issues were identified.

The selection of the starting dose for the first-in-human study is based upon calculating the human equivalent dose and maximum recommended starting dose, in alignment with the principles outlined in the US Food and Drug Administration (FDA) "Guidance for Industry and Reviewers: Estimating the Maximum Safe Starting Dose in Clinical Trials for Therapeutics in Adult Healthy Volunteers (July 2005)."

The initial dose for the first-in-human clinical study was chosen as a single dose of 20 µg of EDP-297. The selection of this dose is based on the results of preclinical 28-day repeat dose toxicology studies (conducted under good laboratory practice) that have been conducted with EDP-297 in mice and dogs.

Subject selection

Male and female subjects of any ethnic origin between the ages of 18 and 65 years with a body mass index of 18–30 kg/m² and a minimum body weight of 50 kg were eligible if they had no clinically relevant abnormality on physical examination, medical history, vital signs, and clinical laboratory testing at screening and admission. Female subjects who were heterosexually active and of childbearing potential agreed to use two effective methods of contraception from screening until 90 days after the last dose of EDP-297. A male subject who had not had a vasectomy and was sexually active with a woman of childbearing potential agreed to use a condom from screening to 90 days after the last dose of study drug.

Exclusion criteria included having high risk factors for contracting coronavirus disease 2019 (COVID-19) or confirmed signs of COVID-19 or a positive test for COVID-19 at admission. In addition, pregnant or nursing women; subjects with clinically relevant evidence or history of illness or disease; positive urine drug screen at screening or day –2; current tobacco smokers or use of tobacco within 1 month prior to screening; regular alcohol consumption; use of prescriptions or non-prescription drugs

or supplements within 14 days prior to study drug; or a clinically significant history of drug sensitivity or allergy were criteria for exclusion. Subjects also with an estimated glomerular filtration rate of <90 ml/min were excluded.¹⁸

Study assessments

Safety and tolerability were evaluated throughout the study including adverse event (AE) monitoring, clinical laboratory (chemistry, hematology, and urinalysis), vital signs (heart rate, respiratory rate, and blood pressure), physical examination, and 12-lead electrocardiogram (ECG).

Blood samples were collected to measure total cholesterol, high-density lipoprotein (HDL), low-density lipoprotein (LDL), and triglycerides.

An itch visual analog scale (VAS) was used to record the intensity of the event.¹⁹ Site personnel instructed the subject to draw a line on the scale corresponding to the maximum intensity of itch. If the VAS score was >0 (i.e., itch), a multidimensional 5-D itch scale was used to assess five different dimensions of pruritus, duration, degree, direction, disability, and distribution.²⁰

For the SAD phase, intensive blood sampling to determine PK parameters occurred over 24 h on day 1 (including predose on day 2), then at 30, 36, 48, 60, 72, 96, and 120 h postdose. Urine samples to assess EDP-297 concentrations were collected from 0 to 6, 6 to 12, 12 to 24, 24 to 48, 48 to 72 h, and 72 to 120 h postdose beginning on day 1. For the MAD phase, intensive sampling occurred over 24 h on day 1 (including predose on day 2) and over 96 h on day 14 (with additional samples in the morning on days 15, 16, 17, and 18) and additional predose samples on days 3, 4, 5, 6, 7, 8, 10, 11, 12, and 13. On days 1 and 14, urine samples to assess EDP-297 concentrations were collected from 0 to 6, 6 to 12, and 12 to 24 h postdose; then on days 15, 16, 17, and 18. Urine samples were collected from 24 to 48 and 48 to 96 h postdose.

EDP-297 and metabolites in human plasma and urine were quantified by high-performance liquid chromatography with tandem mass spectrometric (HPLC-MS/MS) detection. Both plasma and urine assay ranges were 10.0 to 10,000 pg/ml (EDP-297 and EP-030430) and 20.0 to 20,000 pg/ml (EP-030476). The methods were fully validated by assessment of precision, accuracy, sensitivity, and specificity of EDP-297 and metabolites by ICON Bioanalytical Laboratory.

PD measurements included plasma fibroblast growth factor 19 (FGF-19) and serum 7- α -hydroxy-4-cholesten-3-one (C4); blood samples were collected on day –1 and day 1 for the SAD phase, and on day –1, day 1, and day 14 for the MAD phase at predose and 1, 2, 3, 4, 6, 8, 12, and 24 h

postdose. FGF-19 and C4 blood samples were collected on day 1 for the SAD/FE (part 2) phase at predose and 2, 4, 6, 8, 12, and 24 h postdose. Sample collection for BAs was done on day 1 predose and before the evening meal (~8 h postdose).

Bioanalytical methods for PK samples

Bioanalysis for PK samples utilizes a supported liquid extraction with HPLC separation and MS/MS detection for the determination of EDP-297, EP-030430, and EP-030476 in human K2EDTA plasma and urine containing 0.1% Triton X-100 using stable labeled (EP-030674, EP-030921, and EP-030920) as the internal standards, supplied by Enanta Pharmaceuticals (Watertown, MA). A 300 μ l sample aliquot is combined with 25.0 μ l of the working internal standard (4000 pg/ml EP-030674, EP-030921, and EP-030920 in 1% bovine serum albumin [BSA]) and 0.075 ml water. The samples are applied to an Isolute SLE+ 400 μ l 96-well plate. The samples are allowed to absorb onto the sorbent for 5 min. The samples are eluted into a clean plate with two 500 μ l aliquots of ethyl acetate. The samples are evaporated to dryness at ~40°C under a gentle stream of nitrogen. The dried residues are reconstituted in 0.100 ml of 0.1% formic acid in 50:50 acetonitrile: water. Ten (10) microliters are injected onto the LC-MS/MS system. This method was developed and validated at ICON Development Solutions, LLC. Liquid chromatograph utilized a Shimadzu LC-30AD pump on Kinetex 2.6 μ Phenyl-Hexyl 100A 100 \times 2.10 mm column (part number 00D 4495 AN) at 40°C. Mobile phase A contained 0.1% formic acid in water and mobile phase B contained 0.1% formic acid in acetonitrile. The mass spectrometer used was an AB Sciex API 6500 using Turbo Ionspray (positive ion) mode and MS/MS transitions were m/z 646.5/242.1 and m/z 652.5/242.1 for EDP-297 and EP-030430 and their IS EP-030674 and EP-030921 respectively; and m/z 644.4/242.1 and m/z 650.5/242.1 for EP-030476 and IS EP-030920, respectively.

Both plasma and urine assay ranges were 10.0–10,000 pg/ml (EDP-297 and EP-030430) and 20.0–20,000 pg/ml (EP-030476). The cumulative precision (percent coefficient of variation [%CV]) and cumulative accuracy (percentage recovery [%RE]) from the lower limit of quantification (LLOQ) to the upper limit of quantification (ULOQ) were ≤ 6.87 and -2.50 to 2.00 for plasma EDP-297, ≤ 6.10 and -2.50 to 2.00 for plasma EP-030430, ≤ 4.79 and -2.00 to 1.00 for plasma EP-030476, ≤ 5.35 and -2.75 to 1.80 for urine EDP-297, ≤ 7.85 and -2.50 to 2.00 for urine EDP-030430, ≤ 5.52 and -1.39 to 1.50 for urine EP-030476, respectively. The quality control

concentrations were 30.0 pg/ml (low), 3000 pg/ml (medium), and 8000 pg/ml (high) for EDP-297, EP-030430, and EP-030476 in both plasma and urine. Quality control samples were accepted if at least two-thirds of the quality control (QC) samples (with at least 50% at each concentration level) must be within $\pm 15\%$ of the nominal concentrations. The results from the calibration curve standards and QC samples met the acceptance criteria, demonstrating acceptable performance of the method throughout the sample analysis period for both the plasma and urine methods.

Bioanalytical methods for PD samples

Bioanalysis for C4 samples utilizes a supported liquid extraction (SLE) with HPLC separation and MS/MS detection for the determination of C4 in human serum using stable labeled C4-d7 as internal standard. A 100 μ l sample aliquot is combined with 25.0 μ l of the working internal standard (50.0 ng/ml C4-d7 in 1% BSA in water) centrifuged and vortexed and equilibrate. Then, 0.0750 ml of 1% formic acid in water is added to each sample, samples are vortexed, let set to equilibrate, and loaded onto a Strata DE 200 μ l extraction plate. The samples are allowed to absorb for ~5 min before eluting with two 500 μ l portions of n-butyl chloride. The samples are evaporated to dryness at ~40°C under a gentle stream of nitrogen. The dried residues are reconstituted in 0.200 ml of acetonitrile, capped, and vortex mixed. Twenty (20) microliters are injected onto the LC-MS/MS system. This method was validated at ICON Laboratory Services. Liquid chromatograph utilized a Shimadzu LC-20AD pump on Phenomenex, Synergi MAX RP, 4 μ m, 150 \times 2 mm 80A (part #00F-4337-B0) at ambient temperature. Mobile phase A contained 5 mM ammonium acetate in water and mobile phase B contained 5 mM ammonium acetate in methanol. The MS used was an MDS Sciex API 5000 using Turbo Ionspray (positive ion) mode and MS/MS transitions were m/z 401.1/177.1 and m/z 408.5/177.1 for C4 and C4-d7, respectively.

C4 assay range was 0.5–200 ng/ml. The cumulative precision (%CV) and cumulative accuracy (%RE) from LLOQ to ULOQ were ≤ 6.73 and -1.00 to 1.00 . The QC concentrations were 3.44 ng/ml (low), 103 ng/ml (medium), and 153 ng/ml (high). The QC samples were accepted if at least two-thirds of the QC samples (with at least 50% at each concentration level) must be within $\pm 15\%$ of the nominal concentrations. The results from the calibration curve standards and QC samples met the acceptance criteria, demonstrating acceptable performance of the method throughout the sample analysis

period for both plasma and urine methods. A total of 1768 samples were analyzed for C4, with 31 samples below the LLOQ of the assay.

Plasma FGF-19 concentration was measured using a quantitative sandwich enzyme-linked immunosorbent assay (ELISA) technique (FGF19 Quantikine ELISA kit). FGF-19 quantification was done using the SpectraMax (SN: MN02825, NY-120) at ILS-Farmingdale. ICON Laboratory Services analyzed commercially available linearity material for calibration verification, accuracy, linearity, reportable range, and intra-assay precision. Alternate assessment was performed to fulfill proficiency testing requirement. Inter-assay precision was also assessed to test for any variance over five independent analytical runs. A total of 1768 samples were analyzed for FGF-19, with seven samples above the ULOQ of the assay.

Statistical analysis

No formal sample size calculations were performed for this study. The number of subjects participating in each cohort was considered sufficient to characterize the safety, tolerability, PK, and biomarker profiles for the EDP-297 dose level in each phase of the study.

Plasma PK parameters for each dose level were estimated from the concentration–time profiles of EDP-297 and metabolites measured in predose and postdose plasma samples using noncompartmental methods (Phoenix WinNonlin WNL version 8.1). For each treatment, descriptive statistics (number of observations [n], arithmetic mean, geometric mean, SD, %CV, percentage of geometric CV, minimum, median, and maximum) were presented. For time to maximum concentration (T_{\max}), only median, minimum, and maximum were presented.

Dose proportionality was assessed for the SAD phase by comparing maximum concentration (C_{\max}), area under the concentration–time profiles (AUC_{0-t}), and AUC from zero to infinity ($AUC_{0-\infty}$) for EDP-297 across each dose level in the fasted state and for the MAD phase by comparing C_{\max} and AUC for a dosing interval (AUC_{tau}) for EDP-297 across each dose level on day 1 and on day 14. An analysis of variance (ANOVA) was performed on AUC_{0-t} , $AUC_{0-\infty}$, and C_{\max} using the SAS procedure for mixed effects models. The PK parameters were natural logarithm transformed prior to the analysis. The ANOVA model included fixed effects for treatment (fed or fasted), and a random effect for subject. From this model, the back-transformed least-squares means for each treatment were presented. The ratio of the least-squares geometric means of the fed treatment over the

fasted treatment and the corresponding 90% confidence interval (CI) were presented.

RESULTS

Disposition and baseline characteristics

The study was conducted between August 26, 2020, and June 20, 2021. A total of 82 subjects ($n = 42$ in the SAD phase and $n = 40$ in the MAD phase) received at least one dose of EDP-297 or placebo. In the SAD phase, all 10 placebo-treated subjects completed the study; one subject in the EDP-297 100 μg cohort and one in the 600 μg cohort discontinued due to a COVID-19-related positive test and/or exposure. In the MAD phase, all 10 placebo subjects completed the study; one subject in the EDP-297 90 μg cohort discontinued the study due to an AE. Baseline characteristics are summarized in [Table S2](#).

Pharmacokinetics

SAD phase

After administration of EDP-297, individual plasma concentrations above the LLOQ (10 pg/ml) were observed for all doses (fasted and fed) from the first timepoint (0.5 h postdose) onward ([Figure 1](#)). In the fasted state, EDP-297 C_{\max} and AUC_{0-t} increased in a slightly more than dose-proportional manner, whereas dose proportionality was observed for $AUC_{0-\infty}$ ([Table 1](#)). Median T_{\max} ranged from 1.0 h after 100 μg EDP-297 to 2.5 h after 20 μg EDP-297, and mean terminal half-life ($t_{1/2}$) was similar for all doses and ranged from 6.5 h after 60 μg EDP-297 to 10.2 h after 300 μg EDP-297.

In the SAD phase, dose proportionality for EDP-297 was explored using a power model on log-transformed PK parameters ([Table S3](#)). The results suggested a slightly more than dose-proportional increase for C_{\max} , and AUC_{0-t} over the dose range of 20–600 μg . No evidence of deviation from dose proportionality was found for $AUC_{0-\infty}$.

Statistical analysis of the effect of food on the PK profile showed that C_{\max} , AUC_{0-t} , and $AUC_{0-\infty}$ of EDP-297 increased 20%–24% after administration in the fed state compared to the fasted state. Mean T_{\max} for the fed group was longer than the fasted group at 5 h, as compared to 1 h for the fasted group. The ratio of fed/fast was 1.20 for C_{\max} (90% CI: 0.99 to 1.46), 1.24 for $AUC_{0-\infty}$ (90% CI: 1.18 to 1.30), and 1.24 for AUC_{0-t} (90% CI: 1.19 to 1.30).

No substantial amounts of EDP-297 and its metabolites were excreted in urine, indicating that urinary excretion is a minor pathway.

FIGURE 1 Mean EDP-297 plasma concentrations during SAD phase (top) and MAD phase day 1 (middle) and day 14 (bottom), on a semi-log scale (PK population). If more than half of the subjects at a timepoint have values below the LLOQ, the mean has not been presented. LLOQ, lower limit of quantification; MAD, multiple ascending dose; md, multiple doses; PK, pharmacokinetic; SAD, single ascending dose

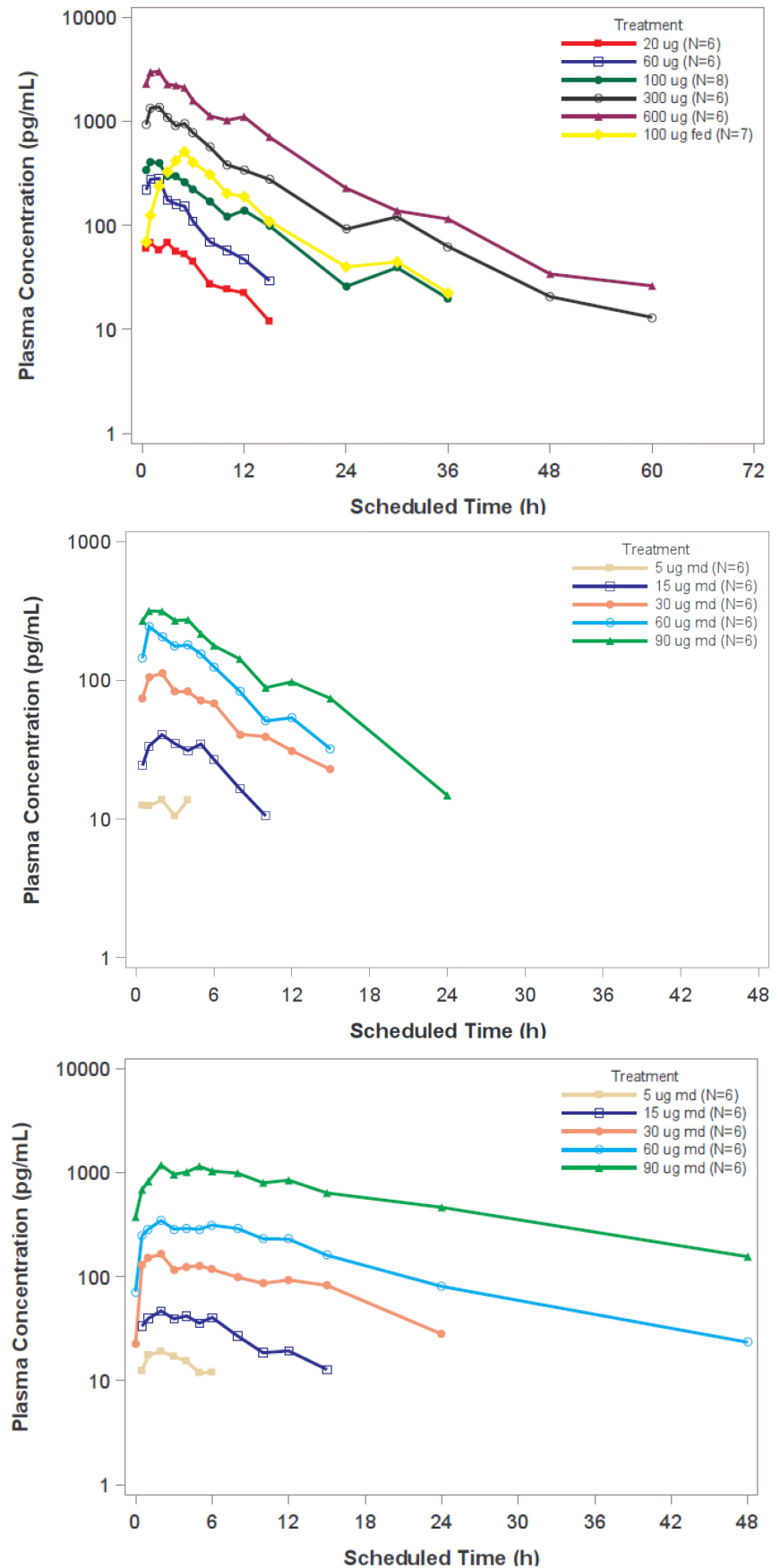


TABLE 1 Plasma PK parameters for EDP-297 during SAD and MAD phases.

SAD PK parameters	100 µg fed					
	20 µg (N = 6)	60 µg (N = 6)	100 µg (N = 8)	(N = 7) ^c	300 µg (N = 6)	600 µg (N = 6)
AUC _{0–inf} , pg/ml*h ^a	780 (252)	2007 (373)	4299 (1480)	5230 (1991)	13,602 (4829)	30,219 (9727)
AUC _{0–24} , pg/ml*h ^a	677 (198)	1820 (223)	3595 (1042)	4452 (1650)	11,494 (3274)	26,988 (7684)
AUC _{0–last} , pg/ml*h ^a	582 (188)	1797 (346)	4044 (1429)	4964 (1938)	13,343 (4842)	29,989 (9643)
C _{max} , pg/ml ^a	78.2 (17.6)	310 (96.2)	477 (153)	552 (162)	1551 (354)	3599 (811)
C ₁₂ , pg/ml ^a	22.4 (11.3)	47.1 (15.4)	139 (44.2)	189 (71.2)	339 (186)	1104 (356)
T _{max} (h) ^b	2.5 (0.5–3.1)	2.0 (0.5–2.0)	1.0 (0.5–2.0)	5.0 (5.0–8.1)	2.0 (1.0–3.0)	1.5 (0.5–3.0)
t _{1/2} , h ^a	8.7 (2.5)	7.4 (4.1)	10.1 (4.2)	9.1 (2.3)	10.4 (1.9)	8.4 (2.3)
CL/F, L/h ^a	29.0 (13.0)	30.8 (5.6)	26.1 (9.8)	22.1 (9.6)	24.1 (7.2)	21.7 (7.4)
MAD PK parameters	15 µg q.d.					
	5 µg q.d. (N = 6)	(N = 6)	30 µg q.d. (N = 6)	60 µg q.d. (N = 6)	90 µg q.d. (N = 6)	
<i>Day 1</i>						
AUC _{0–tau} , pg/ml*h ^a	184 (48.3)	358 (107)	986 (56.9)	1781 (343)	2886 (583)	
C _{max} , pg/ml ^a	18.6 (5.2)	42.0 (3.7)	120 (31.1)	270 (72.6)	360 (86.5)	
C ₁₂ , pg/ml ^a	LLOQ	9.8 (7.9)	31.0 (13.7)	53.6 (18.8)	97.3 (18.3)	
T _{max} , h ^b	1.5 (0.5–4.0)	2.1 (1.0–5.0)	1.5 (1.0–6.0)	1.5 (1.0–5.0)	1.5 (1.0–2.0)	
<i>Day 14</i>						
AUC _{0–tau} , pg/ml*h ^a	252 (88.9)	524 (105)	2022 (1023)	4911 (3398)	18,384 (13749)	
C _{max} , pg/ml ^a	19.8 (5.6)	52.2 (6.7)	191 (54.5)	399 (159)	1235 (839)	
C _{min} , pg/ml ^a	LLOQ	LLOQ	28.1 (24.9)	80.5 (82.3)	463 (392)	
C ₁₂ , pg/ml ^a	LLOQ	19.3 (6.8)	92.7 (67.8)	229 (209)	845 (748)	
T _{max} , h ^b	2.0 (1.0–4.0)	2.0 (0.5–6.0)	2.0 (0.5–5.0)	2.0 (0.5–8.0)	2.0 (2.0–8.0)	
t _{1/2} , h ^a	9.4 (4.5)	9.2 (3.3)	9.1 (3.4)	9.8 (4.1)	12.7 (3.1)	
CL/F, L/h ^a	21.7 (7.4)	29.6 (5.8)	18.0 (8.1)	18.3 (11.6)	7.1 (4.0)	
Accumulation ratio ^c	1.4 (0.3)	1.5 (0.3)	2.1 (1.1)	2.6 (1.5)	6.1 (3.8)	

Abbreviations: AUC_{0–24}, 0–24-hour area under the concentration–time curve; AUC_{0–inf}, area under the concentration–time curve from zero to infinity; AUC_{0–last}, area under the concentration–time curve from time of administration up to the time of the last quantifiable concentration; CL/F, total apparent clearance; C_{max}, maximum concentration; C_{min}, minimum concentration; MAD, multiple ascending dose; PK, pharmacokinetic; SAD, single ascending dose; t_{1/2}, terminal half-life; T_{max}, time to maximum concentration.

^aData presented as mean (SD).

^bData presented as median (range).

^cAccumulation ratio based on AUC_{0–24}.

MAD phase

After administration of the first dose of EDP-297, plasma concentrations were measurable from the first timepoint (0.5 h) onward for all subjects, except for the 5 µg dose where measurable plasma concentrations for all subjects were first obtained at 4 h postdose (Figure 1). Predose samples on days 2 to 14 showed no values above the LLOQ after administration of 5 µg EDP-297 and very limited values above the LLOQ after administration of 15 µg EDP-297. For 30 µg EDP-297 and higher, trough levels increased with time and dose (Table 1). After administration of EDP-297 on day 14, C_{max} of EDP-297 were measured at 2 h postdose for all doses. Mean t_{1/2} was similar for doses between

5 µg and 60 µg, ranging between 8.5 and 9.1 h and slightly higher after 90 µg EDP-297 (12.5 h). After administration of EDP-297 for 14 days, geometric mean accumulation index increased from 1.34 with 5 µg EDP-297 to 5.34 with 90 µg.

Dose proportionality analysis for EDP-297 for day 1 suggested a dose-proportional increase for C_{max} and AUC_{0–tau} (Table S3). The results on day 14 suggested a more than dose-proportional increase for C_{max} and AUC_{0–tau}.

After dosing with EDP-297, plasma concentrations of the EP-030430 metabolite were not observed in any subject at any dose level tested in the SAD or MAD phases; plasma concentrations of the metabolite EP-030476 could only be detected in at least one subject at the two highest single doses tested (300 µg or 600 µg EDP-297).

Pharmacodynamics

On day 7 and day 14, mean C4 AUC_{0-24} decreased from baseline as the dose of EDP-297 increased in both the SAD and MAD phases, respectively, with $\geq 50\%$ target engagement for multiple doses of $30\mu\text{g}$ and higher, and up to a 91.7% decrease from baseline at the highest multiple dose of $90\mu\text{g}$ (Figure 2). Mean C4 minimum concentration (C_{min}) decreased as the dose of EDP-297 was increased, with $\geq 50\%$ target engagement for multiple doses of $30\mu\text{g}$ and higher, and up to a 95.1% decrease from baseline at the highest multiple dose of $90\mu\text{g}$ (Table S4). The two lowest doses (5 and $15\mu\text{g}$) were not associated with pruritus, and resulted in modest C4 target engagement ($< 50\%$).

Mean FGF-19 AUC_{0-24} generally increased as doses of EDP-297 were increased in both the SAD and MAD

phases, with a 94.7% increase from baseline observed at the highest multiple dose of $90\mu\text{g}$ (Figure 2). Mean FGF-19 C_{max} showed no clear dose response as EDP-297 doses were increased, with a 64.5% increase from baseline observed at multiple doses of $15\mu\text{g}$ (Table S4).

Alkaline phosphatase (ALP) mean concentrations in the MAD phase increased from baseline over time. Notable mean increases were observed at MAD $30\mu\text{g}$ with a mean baseline of 64.8 IU/L increased to a maximum of 86.3 IU/L on day 17, at MAD $60\mu\text{g}$ with a mean baseline of 55.3 IU/L increased to a maximum of 77.2 on day 16, at MAD $90\mu\text{g}$ with a mean baseline of 74.3 IU/L increased to a maximum of 117.4 on day 16. ALP values did not show clinical differences in the SAD phase.

Gamma-glutamyl transpeptidase (GGT) mean concentrations in the MAD phase decreased from baseline over

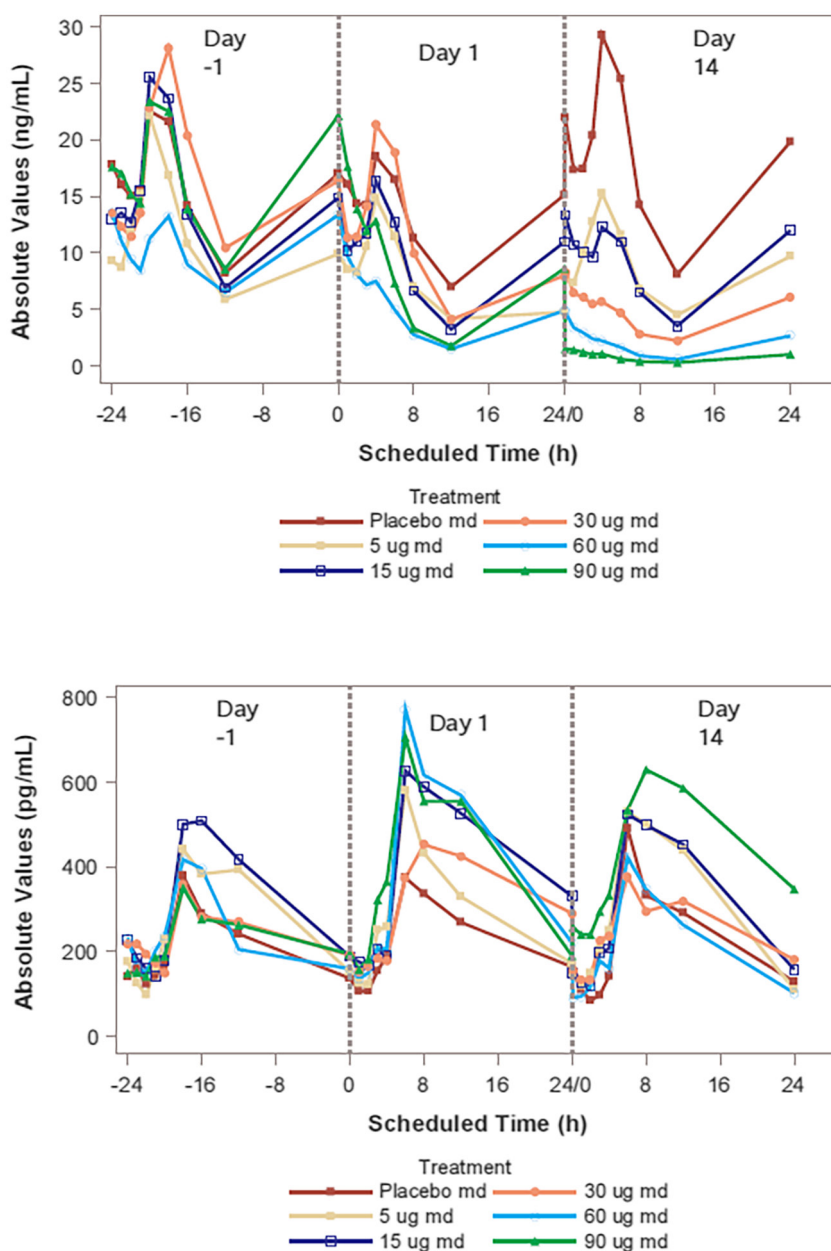


FIGURE 2 Mean C4 (top) and FGF-19 (bottom) arithmetic mean serum levels versus time on a linear scale MAD phase (PD population). MAD, multiple ascending dose; md, multiple doses; PD, pharmacodynamic

TABLE 2 Incidence of TEAEs during SAD and MAD phases

SAD phase	Pooled placebo fasted (N = 10)	20 µg fasted (N = 6)	60 µg fasted (N = 6)	100 µg fasted (N = 8)	300 µg fasted (N = 6)	600 µg fasted (N = 6)	Placebo fed (N = 2)	100 µg fed (N = 7)
At least one TEAE [number of TEAEs]	7 (70.0) [14]	4 (66.7) [9]	2 (33.3) [3]	4 (50.0) [9]	5 (83.3) [20]	5 (83.3) [10]	2 (100.0) [4]	2 (28.6) [4]
Drug-related TEAE	1 (10.0)	2 (33.3)	0	0	2 (33.3)	3 (50.0)	0	0
Headache	1 (10.0)	0	0	0	2 (33.3)	1 (16.7)	0	0
Dizziness	0	0	0	0	2 (33.3)	0	0	0
Hematoma	0	0	0	0	2 (33.3)	0	0	0
Myalgia	1 (10.0)	2 (33.3)	1 (16.7)	0	1 (16.7)	0	0	0
Dyspnea	2 (20.0)	0	0	0	0	0	0	0
Pruritus	1 (10.0)	0	0	0	2 (33.3)	2 (33.3)	0	0
MAD phase	Pooled placebo fasted (N = 10)	5 µg q.d. fasted (N = 6)	15 µg q.d. fasted (N = 6)	30 µg q.d. fasted (N = 6)	60 µg q.d. fasted (N = 6)	90 µg q.d. fasted (N = 6)		
At least one TEAE [number of TEAEs]	7 (70.0) [19]	3 (50.0) [4]	4 (66.7) [5]	6 (100.0) [23]	6 (100.0) [26]	6 (100.0) [16]		
Discontinued for TEAE	0	0	0	0	0	0		1 (16.7)
Drug-related TEAE	0	0	0	2 (33.3)	1 (16.7)	4 (66.7)		
Abdominal discomfort	1 (10.0)	0	0	3 (50.0)	1 (16.7)	1 (16.7)		1 (16.7)
Headache	0	1 (16.7)	1 (16.7)	4 (66.7)	2 (33.3)	1 (16.7)		1 (16.7)
Fatigue	2 (20.0)	0	0	0	0	1 (16.7)		0
Catheter site related reaction	2 (20.0)	0	0	3 (50.0)	0	0		1 (16.7)
Vessel puncture site thrombosis	0	0	0	0	0	2 (33.3)		0
Medical device site reaction	0	0	0	2 (33.3)	1 (16.7)	0		0
Arthralgia	0	0	0	2 (33.3)	0	0		0
Pruritus	2 (20.0)	0	0	1 (16.7)	2 (33.3)	4 (66.7)		4 (66.7)
Dry skin	2 (20.0)	0	0	0	3 (50.0)	0		0

Abbreviations: MAD, multiple ascending dose; SAD, single ascending dose; TEAE, treatment-emergent adverse event.

time. Notable mean increases were observed at MAD 30 μg with a mean baseline of 20.7 IU/L decreased to a minimum 12.0 IU/L on day 15, at MAD 60 μg with a mean baseline of 10.3 IU/L decreased to a minimum 6.0 IU/L on days 8 and 9, at MAD 90 μg with a mean baseline 18.8 IU/L decreased to a minimum 13.0 IU/L on days 11 and 14. GGT values did not show clinical differences in the SAD phase.

No clear dose-related effect of EDP-297 was observed on BAs at any dose in the SAD or MAD phases.

Safety/tolerability

EDP-297 was generally well-tolerated following single and multiple doses for 14 days except at the highest MAD dose (90 μg ; Table 2). No serious AEs or discontinuations due to treatment-emergent adverse events (TEAEs) occurred in the SAD phase; one subject in the 90 μg cohort of the MAD phase discontinued because of pruritus. In the SAD phase, five (11.9%) subjects reported TEAEs of moderate severity, including 20 μg group (1 [16.7%] subject; myalgia and back pain), 300 μg group (3 [50.0%] subjects; headache, dizziness, syncope, and pruritus), and in the placebo group (1 [10.0%] subject; headache). Most TEAEs were not related/unlikely related to study drug. Pruritus in five (11.9%) subjects was the most common TEAE considered possibly related to drug therapy, with four in the EDP-297 arms and one in the placebo arm.

In the MAD phase, all TEAEs were mild except for five subjects with moderate pruritus ($n = 1$, 30 μg) and severe pruritus ($n = 4$, 90 μg). Pruritus was observed at multiple

doses $\geq 30 \mu\text{g}$ with discontinuation ($n = 1$) due to pruritus in the highest MAD cohort (90 μg). Although within the dosing groups, subjects with pruritus did not show a consistently different PK from subjects without pruritus, pruritus only occurred at the two highest dose levels. Overall, the incidence of pruritus increased with increasing doses, and appeared dose dependent at doses $> 30 \mu\text{g}$. Although the finding was based on a small number of subjects, differences in exposure to EDP-297 (C_{max} and AUC) were observed mainly after multiple dosing and at the 90 μg multiple dose (Table 3): Subjects with pruritus showed up to 2.4-fold higher AUC levels for EDP-297 than subjects without pruritus (90 μg).

No clinically significant abnormal safety laboratory or abnormal ECG findings occurred, except for one subject with a grade 2 ALT elevation in the MAD 90 μg dose that was not associated with other liver enzyme abnormalities. No clinically meaningful changes in the lipid profile were observed, except for a trend toward a decrease in HDL-cholesterol and increase in LDL-cholesterol in the MAD cohort at the 90 μg dose. Mean lipids values were within the normal range during the entire course of the study (Figure 3).

DISCUSSION

In this study, EDP-297, a selective FXR agonist, was safe and well-tolerated with time-linear PKs supporting once daily oral dosing, target engagement, and no food effect. In the SAD phase, $\text{AUC}_{0-\text{inf}}$ was dose proportional based on the power model assessment, and AUC_{0-t} was slightly

TABLE 3 Summary of PK parameters for EDP-297 in plasma on day 1 and day 14 with and without pruritus – MAD (PK set)

Dose (μg)	Median C_{max} (pg/ml)		Median $\text{AUC}_{0-\text{tau}}$ (h*pg/ml)	
	Pruritus [n]	NO pruritus [n]	Pruritus	NO pruritus
<i>Day 1</i>				
5	n/a [0]	19 [6]	n/a	167
15	n/a [0]	43 [6]	n/a	345
30	96.8 [1]	139 [5]	918	975
60	304 [2]	256 [4]	1861	1810
90	340 [4]	420 [2]	3137	2710
<i>Day 14</i>				
5	n/a [0]	17 [6]	n/a	239
15	n/a [0]	53 [6]	n/a	505
30	234 [1]	160 [5]	3760	1426
60	445 [2]	305 [4]	6220	2460
90	1288 [3]	745 [2]	24,167	9037

Abbreviations: $\text{AUC}_{0-\text{tau}}$, area under the concentration curve for a dosing interval; C_{max} , maximum concentration; MAD, multiple ascending dose; n/a, not applicable; PK, pharmacokinetic.

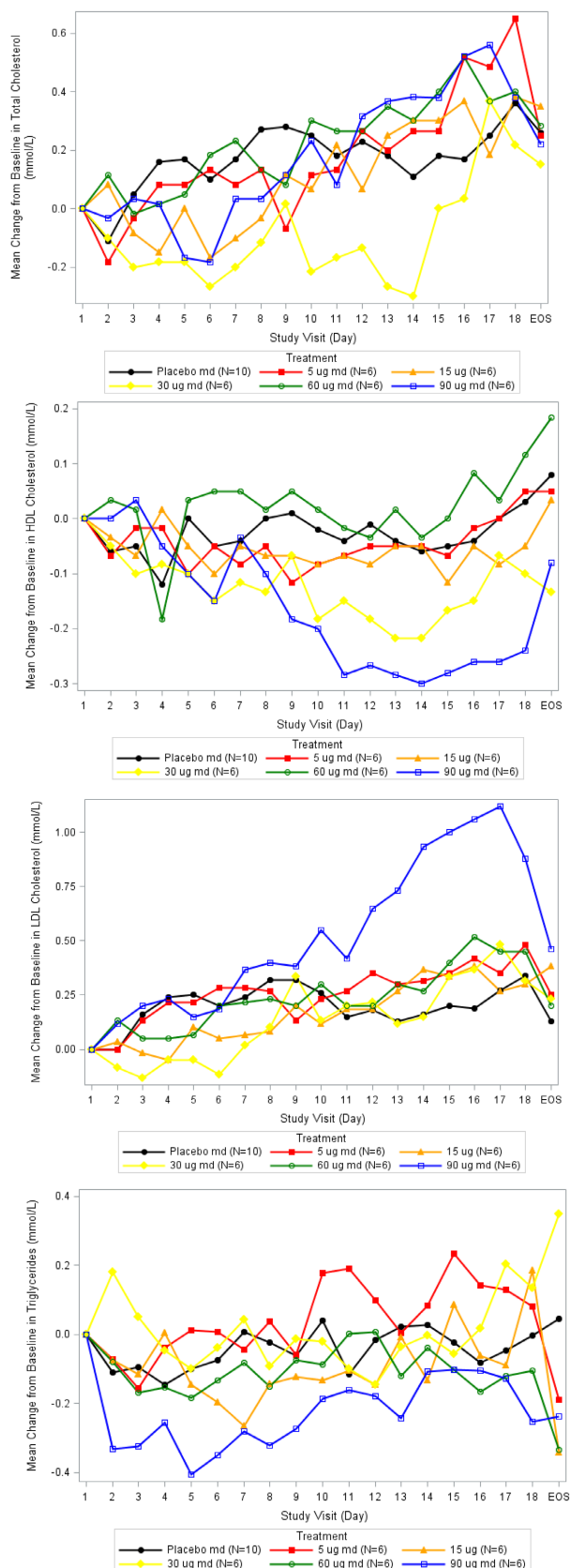


FIGURE 3 Mean change from baseline for total cholesterol, HDL-cholesterol, LDL-cholesterol, and triglycerides over time.

more than dose proportional, with slopes of 1.09 and 1.17 for $AUC_{0-\infty}$ and AUC_{0-t} , respectively. Following single doses, $AUC_{0-\infty}$ is a more complete measure of extent of exposure and generally reflects a better assessment of dose proportionality.

Overall, EDP-297 PK was dose proportional following single doses on day 1 and following multiple doses based on AUC, however, a more than dose proportional increase was observed in the MAD phase on day 14. Which was mainly due to the change in the PK characteristics at the 90 μ g dose. The accumulation ratio for doses <60 μ g ranged from 1.34 to 2.28, which is generally in line with what would be expected based on the overall PK profile. However, the accumulation ratio at the 90 μ g dose was 5.34, which is higher than what would be expected based on the PK characteristics. In summary, the more than dose proportional increase at day 14 is driven by the 90 μ g dose, which was not as well-tolerated and had a different PK profile than lower doses. The reason for this increase in accumulation at 90 μ g is not known.

Overall, EDP-297 was well-tolerated except for pruritus and liver enzyme elevations observed especially at the 90 μ g dose in the MAD phase. Pruritus was observed at single doses ≥ 300 μ g and multiple doses ≥ 30 μ g. One subject in the 90 μ g MAD cohort experienced a grade 2 elevation in ALT levels that was not associated with other changes in liver enzymes that was also associated with severe pruritus. EDP-297 exposure increased with increasing single and multiple doses, with a time-linear PK profile. Strong FXR target engagement was demonstrated following multiple doses, with an increase in FGF-19 and a decrease in C4 levels of up to 95% and 92%, respectively. EDP-297 metabolites only measurable at low concentrations and are unlikely to contribute to the pharmacological effects of the parent drug. Minimal urinary concentrations of EDP-297 suggest that urinary excretion is a minor route of elimination.

Whereas FXR agonists improve hepatic fibrosis, inflammation, and liver cell injury, their use often is limited by safety and tolerability issues, such as pruritus, liver function abnormalities, and unwelcome alterations in the lipid profile.²¹ Second generation FXR agonists are being developed to reduce treatment-limiting side effects while retaining beneficial effects on NASH.²² For instance, EDP-305 resulted in lower increases in LDL cholesterol compared to obeticholic acid^{21,23} or aldafermin.²⁴ Cilofexor produced modest increases in LDL cholesterol, however, reductions in hepatic fat and ALT also were more modest.²⁵ ALT increases have also been observed with other phase I FXR agonist studies in healthy volunteers, including EDP-305 and tropifexor.²⁶ Increases in LDL with

FXR agonists appear to be a class effect.²⁷ The impact of elevated LDL and reduced HDL concentrations with FXR agonists on long-term cardiovascular risk remains to be determined,^{28,29} however, it appears that newer FXR agonists induce more modest lipid alterations than earlier FXR agonists. Although LDL levels were increased and HDL levels were decreased in this study, no clinically meaningful changes were observed and mean lipid levels remained within the normal range.

Pruritus is an important tolerability concern with FXR agonists resulting in treatment discontinuation in 9% of patients in a large, 18-month trial of obeticholic acid.²¹ However, pruritus occurs commonly in patients with NASH with reports of a 20% incidence at baseline.^{22,30} Even within clinical studies of FXR agonists, the incidence of pruritus at baseline and in placebo treatment groups is ~20%.²² Phase I studies in healthy volunteers have shown similar pruritus effects at higher multiple dose cohorts, including MET409 at 100mg and 150mg MAD (14 days), EDP-305 20 mg, and 10 mg MAD (14 days), and HPG1860 at 20 mg MAD (14 days).³¹⁻³³ Studies with second-generation FXR agonists including tropifexor³⁴ and MET409³⁵ as well as first-generation FXR agonists indicate that pruritus is a class effect, and a dose-dependent increase in the incidence of pruritus is apparent.²⁵ A similar trend for a dose-dependent increase in the incidence of pruritus was observed in this study with EDP-297.

Increases in circulating FGF-19 levels and decreases in C4 levels are PD markers of FXR agonist target engagement.³⁶ Consistent with FXR target engagement, FGF-19 levels increased and C4 levels decreased from baseline during a 12-week study with EDP-305,³⁷ as well as in a 24-week study with cilofexor,²⁵ which is similar to effects observed with other FXR agonists. PD effects indicative of FXR activation have shown a more pronounced effect in patients with presumptive NAFLD and NASH when compared with healthy subjects.^{25,31,37-39} In this study with EDP-297, target engagement was confirmed by decreases in C4 levels and increases in FGF-19 levels during 14 days of treatment. Increases in liver enzyme levels have been observed with other FXR agonists. In this study, only one subject at the highest dose in the MAD phase experienced an elevated ALT level that was not associated with other enzyme elevations. This study also showed increases in ALP and decreases in GGT, which is also consistent with FXR engagement in healthy volunteers. Furthermore, patients with NASH are reported to have a different metabolic profile than healthy subjects, and plasma exposures in patients with NASH are usually higher than healthy subjects,⁴⁰ which may contribute to more pronounced PD effects compared with healthy subjects.

In summary, this first-in-human study of EDP-297 demonstrates a PK profile that supported once daily dosing and a target engagement as evidenced by changes in FGF-19 and C4 levels. These results aid in determining the optimal EDP-297 dose that would lead to a PK/PD profile supporting once daily dosing with an acceptable tolerability (i.e., minimal incidence of pruritus and lipids elevation).

AUTHOR CONTRIBUTIONS

C.M. wrote the manuscript. A.A., C.M., E.L., and N.A. designed the research. J.O. and S.vM. performed the research. A.A., C.M., E.L., J.O., S.vM., and N.A. analyzed the data.

ACKNOWLEDGMENTS

The authors would like to thank all volunteers, investigators, and study personnel who participated in the clinical studies. The authors acknowledge the editorial assistance of Richard S. Perry, PharmD, in the preparation of this manuscript, which was supported by Enanta Pharmaceuticals, Inc., Watertown, MA.

FUNDING INFORMATION

The study was funded by Enanta Pharmaceuticals, Inc. and was designed in conjunction with the authors. Enanta was involved in study design, data collection, data analysis, data interpretation, and writing of the report. All authors had full access to all the data in the study, participated in drafting and editing the manuscript, and were responsible for the decision to submit for publication.

CONFLICT OF INTEREST

C.M., A.A., E.L., and N.A. are employees of and have held stock in Enanta Pharmaceuticals, Inc., Watertown, MA, at the time of this study. J.O. and S.V. are employees of PRA (ICON). All authors declared no competing interests for this work.

REFERENCES

1. Alemi F, Kwon E, Poole DP, et al. The TGR5 receptor mediates bile acid-induced itch and analgesia. *J Clin Invest.* 2013;123:1513-1530.
2. Lieu T, Jayaweera G, Zhao P, et al. The bile acid receptor TGR5 activates the TRPA1 channel to induce itch in mice. *Gastroenterology.* 2014;147:1417-1428.
3. Anisfeld AM, Kast-Woelbern HR, Lee H, Zhang Y, Lee FY, Edwards PA. Activation of the nuclear receptor FXR induces fibrinogen expression: a new role for bile acid signaling. *J Lipid Res.* 2005;46:458-468.
4. McMahan RH, Wang XX, Cheng LL, et al. Bile acid receptor activation modulates hepatic monocyte activity and improves non-alcoholic fatty liver disease. *J Biol Chem.* 2013;288:11761-11770.

5. Adorini L, Pruzanski M, Shapiro D. Farnesoid X receptor targeting to treat nonalcoholic steatohepatitis. *Drug Discov Today*. 2012;17(17-18):988-997.
6. Hollman DA, Milona A, van Erpecum KJ, van Mil SW. Anti-inflammatory and metabolic actions of FXR: insights into molecular mechanisms. *Biochim Biophys Acta*. 2012;1821(11):1443-1452.
7. Watanabe M, Houten SM, Wang L, et al. Bile acids lower triglyceride levels via a pathway involving FXR, SHP, and SREBP-1c. *J Clin Invest*. 2004;113(10):1408-1418.
8. Zhao K, He J, Zhang Y, et al. Activation of FXR protects against renal fibrosis via suppressing Smad3 expression. *Sci Rep*. 2016;6:37234.
9. Xu JY, Li ZP, Zhang L, Ji G. Recent insights into farnesoid X receptor in non-alcoholic fatty liver disease. *World J Gastroenterol*. 2014;20(37):13493-13500.
10. Sinal CJ, Tohkin M, Miyata M, Ward JM, Lambert G, Gonzalez FJ. Targeted disruption of the nuclear receptor FXR/BAR impairs bile acid and lipid homeostasis. *Cell*. 2000;102(6):731-744.
11. Calkin AC, Tontonoz P. Transcriptional integration of metabolism by the nuclear sterol-activated receptors LXR and FXR. *Nat Rev Mol Cell Biol*. 2012;13(4):213-224.
12. Lambert G, Amar MJ, Guo G, Brewer HB Jr, Gonzalez FJ, Sinal CJ. The farnesoid X-receptor is an essential regulator of cholesterol homeostasis. *J Biol Chem*. 2003;278(4):2563-2570.
13. Makishima M, Okamoto AY, Repa JJ, et al. Identification of a nuclear receptor for bile acids. *Science*. 1999;284(5418):1362-1365.
14. Parks DJ, Blanchard SG, Bledsoe RK, et al. Bile acids: natural ligands for an orphan nuclear receptor. *Science*. 1999;284(5418):1365-1368.
15. Wang H, Chen J, Hollister K, Sowers LC, Forman BM. Endogenous bile acids are ligands for the nuclear receptor FXR/BAR. *Mol Cell*. 1999;3(5):543-553.
16. Chau M, Roqueta-Rivera M, Wang G, et al. A novel FXR agonist EDP-297 exerts anti-inflammatory and hepatoprotective effects in human liver 3D microtissues and in rodent models of liver injury and NASH. *J Hepatol*. 2020;73:S672.
17. Sojoodi M, Wang Y, Erstad D, et al. EDP-297, a novel and potent fxr agonist, exhibit robust anti-fibrotic effects with significant liver function in a rat model of non-alcoholic steatohepatitis. *J Hepatol*. 2020;73:S453.
18. Levey AS, Stevens LA, Schmid CH, et al. A new equation to estimate glomerular filtration rate. *Ann Intern Med*. 2009;150(9):604-612.
19. Furue M, Ebata T, Ikoma A, et al. Verbalizing extremes of the visual analogue scale for pruritus. *Acta Derm Venereol*. 2013;93(2):214-215.
20. Elman S, Hynan LS, Gabriel V, Mayo MJ. The 5-D itch scale: a new measure of pruritus. *Br J Dermatol*. 2010;162(3):587-593.
21. Younossi ZM, Ratzliff V, Loomba R, et al. Obeticholic acid for the treatment of non-alcoholic steatohepatitis: interim analysis from a multicentre, randomised, placebo-controlled phase 3 trial. *Lancet*. 2019;394(10215):2184-2196.
22. Kremoser C. FXR agonists for NASH: how are they different and what difference do they make? *J Hepatol*. 2021;75(1):12-15.
23. Neuschwander-Tetri BA, Loomba R, Sanyal AJ, et al. Farnesoid X nuclear receptor ligand obeticholic acid for non-cirrhotic, non-alcoholic steatohepatitis (FLINT): a multicentre, randomised, placebo-controlled trial. *Lancet*. 2015;385(9972):956-965.
24. Rinella ME, Trotter JF, Abdelmalek MF, et al. Rosuvastatin improves the FGF19 analogue NGM282-associated lipid changes in patients with non-alcoholic steatohepatitis. *J Hepatol*. 2019;70(4):735-744.
25. Patel K, Harrison SA, Elkashab M, et al. Cilofexor, a nonsteroidal FXR agonist, in non-cirrhotic patients with nonalcoholic steatohepatitis: a phase 2 randomized controlled trial. *Hepatology*. 2020;72(1):58-71.
26. Badman MK, Chen J, Desai S, et al. Safety, tolerability, pharmacokinetics, and pharmacodynamics of the novel non-bile acid FXR agonist Tropifexor (LJN452) in healthy volunteers. *Clin Pharmacol Drug Dev*. 2020;9(3):395-410.
27. Papazyan R, Liu X, Liu J, et al. FXR activation by obeticholic acid or nonsteroidal agonists induces a human-like lipoprotein cholesterol change in mice with humanized chimeric liver. *J Lipid Res*. 2018;59(6):982-993.
28. Pockros PJ, Fuchs M, Freilich B, et al. CONTROL: A randomized phase 2 study of obeticholic acid and atorvastatin on lipoproteins in nonalcoholic steatohepatitis patients. *Liver Int*. 2019;39(11):2082-1093.
29. Siddiqui MS, Van Natta ML, Connelly MA, et al. Impact of obeticholic acid on the lipoprotein profile in patients with non-alcoholic steatohepatitis. *J Hepatol*. 2020;72(1):25-33.
30. Boehlig A, Gerhardt F, Petroff D, et al. Prevalence of pruritus and association with anxiety and depression in patients with nonalcoholic fatty liver disease. *Biomedicine*. 2022;10(2):451. doi:10.3390/biomedicines10020451
31. Ahmad A, Sanderson K, Dickerson D, Adda N. Phase 1 study of EDP-305, a novel once-daily oral farnesoid × receptor agonist, in healthy subjects and those with presumptive nonalcoholic fatty liver disease. *Int J Gastroenterol*. 2021;5(2):68-79. doi:10.11648/j.ijg.20210502.16
32. Chen H, Cremer K, Bischoff E, et al. MET409, an optimized sustained FXR agonist, was safe and well-tolerated in a 14-day phase 1 study in healthy subjects. *J Hepatol*. 2019;70(1):E789.
33. HPG1860. Press release, Hepagene Therapeutics, 23 August 2021.
34. Pedrosa M, Seyedkazemi S, Francque S, et al. A randomized, double-blind, multicenter, phase 2b study to evaluate the safety and efficacy of a combination of tropifexor and cenicriviroc in patients with nonalcoholic steatohepatitis and liver fibrosis: study design of the TANDEM trial. *Contemp Clin Trials*. 2020;88:105889.
35. Harrison SA, Bashir MR, Lee KJ, et al. A structurally optimized FXR agonist, MET409, reduced liver fat content over 12 weeks in patients with non-alcoholic steatohepatitis. *J Hepatol*. 2021;75(1):25-33.
36. Thomas C, Pellicciari R, Pruzanski M, Auwerx J, Schoonjans K. Targeting bile-acid signalling for metabolic diseases. *Nat Rev Drug Discov*. 2008;7(8):678-693.
37. Ratzliff V, Rinella ME, Neuschwander-Tetri BA, et al. EDP-305 in patients with NASH: A phase II double-blind placebo-controlled dose-ranging study. *J Hepatol*. 2022;76(3):506-517.
38. Ahmad A, Adda N. Assessment of drug-drug interaction potential with EDP-305, a farnesoid X receptor agonist, in healthy subjects. *Clin Transl Sci*. 2022;15(9):2146-2158. doi:10.1111/cts.13348
39. Myers RP, Djedjos C, Kirby B, et al. Pharmacodynamic effects of the oral, non-steroidal farnesoid X receptor agonist GS-9674 in healthy volunteers. *J Can Assoc Gastroenterol*. 2018;1(Suppl 1):346. doi:10.1093/jcag/gwy008.199

40. Jamwal R, de la Monte SM, Ogasawara K, Adusumalli S, Barlock BB, Akhlaghi F. Nonalcoholic fatty liver disease and diabetes are associated with decreased CYP3A4 protein expression and activity in human liver. *Mol Pharm*. 2018;15(7):2621-2632.

SUPPORTING INFORMATION

Additional supporting information can be found online in the Supporting Information section at the end of this article.

How to cite this article: Marotta C, Ahmad A, Luo E, Oosterhaven J, van Marle S, Adda N. EDP-297: A novel, farnesoid X receptor agonist—Results of a phase I study in healthy subjects. *Clin Transl Sci*. 2023;16:338-351. doi:[10.1111/cts.13453](https://doi.org/10.1111/cts.13453)